Method for the determining of the spatial distribution of noble metals on porous solids by complex formation with tris(methoxyphenyl)phosphine and ^{31}P MAS NMR

Spectroscopic background: Due to the high reactivity of tris(methoxyphenyl)phosphine (P(PhOMe)$_3$) in the complex formation with noble metals (NM: Pt, Rh, Pd, Ru) and the molecular diameter of 0.97 nm, this molecule is suitable for determining the presence of noble metals at the outer particle surface of microporous zeolites, such as zeolite Y (structure type FAU), since the micropores and cages, such as the 12-ring pores of this zeolite with a diameter of 0.74 nm, are not accessible for this molecule. On amorphous silica (A200 or A300) and mesoporous SBA-15, on the other hand, all well-dispersed noble metal atoms are available for complex formation with P(PhOMe)$_3$ due to the open surfaces and large pores of these materials (see **Fig. 1**) [1].

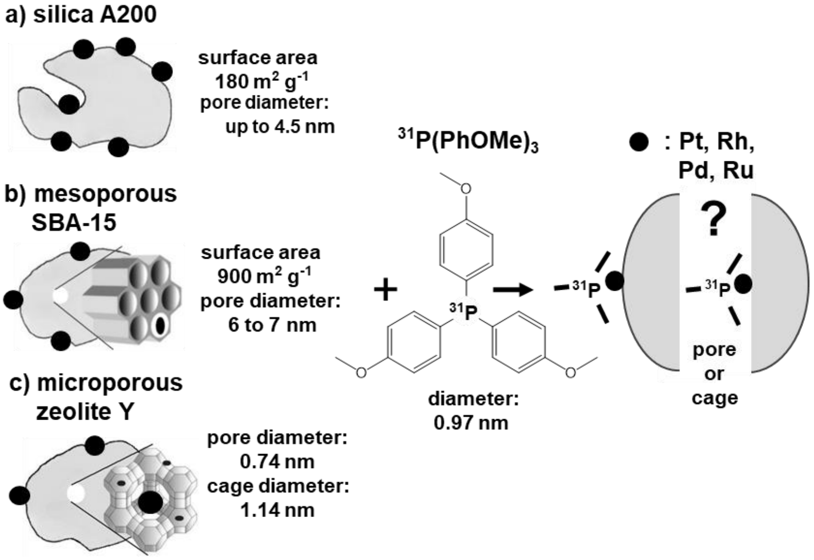

Fig. 1

Because of the natural abundance of 100% and a nuclear spin of $I = ½$ of the ^{31}P isotope, quantitative ^{31}P MAS NMR spectroscopy is a suitable tool for the investigation of P(PhOMe)$_3$ complexes formed at noble metals on porous supports with high sensitivity. While bulk P(PhOMe)$_3$ causes a narrow ^{31}P MAS NMR signal at δ_{31P} = -14 ppm (Table 1 in [1]), physisorption of this molecule on open silica surfaces and in mesopores leads to a low-field resonance shift to δ_{31P} = -10 ppm (**Fig. 2a** shown below and Fig. 1, right-hand side, in Ref. [1]). Same types of ^{31}P MAS NMR signals are observed for adsorption of P(PhOMe)$_3$ on zeolite H-Y (**Fig. 2b** shown below and Fig. 1, right-hand side, in Ref. [1]). The latter finding indicates that $P(PhOMe)_3$, in contrast to PPh_3 (see Fig. 2e in the Section “method 21”), is not able to enter the supercages of zeolite Y and to interact with the Broensted acidic bridging OH groups (Si(OH)Al) located in these cages.

^{31}P HPDEC MAS NMR

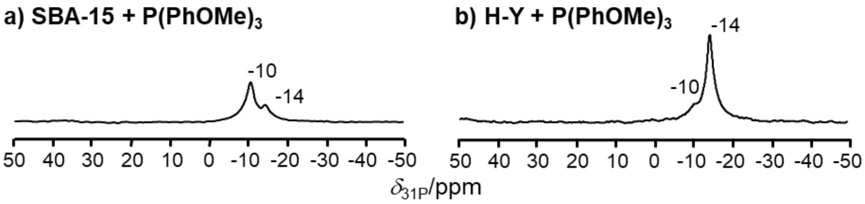

a) SBA-15 + $P(PhOMe)_3$

b) H-Y + $P(PhOMe)_3$

Fig. 2

For studying the complex formation of $P(PhOMe)_3$ with noble metals, H_2-reduced Pt-, Rh-, Pd-, and Ru-loaded meso- and microporous support materials were prepared as described in Refs. [1-5]. In their H_2-reduced state, these catalysts demonstrated a high activity in the hydrogenation of propene and the dehydrogenation of propane [4, 5]. The complex formation of $P(PhOMe)_3$ with noble metals, such as platinum and rhodium, on the silica A200 with a well accessible surface on mesoporous SBA-15 leads to broad ^{31}P MAS NMR signals at δ_{31P} ca. 35 ppm, which is a similar chemical shift range as observed for complexes formed by adsorption of PPh_3 (compare left- and right-hand side of **Fig. 3** shown below and Fig. 2 in Ref. [1]).

^{31}P HPDEC MAS NMR

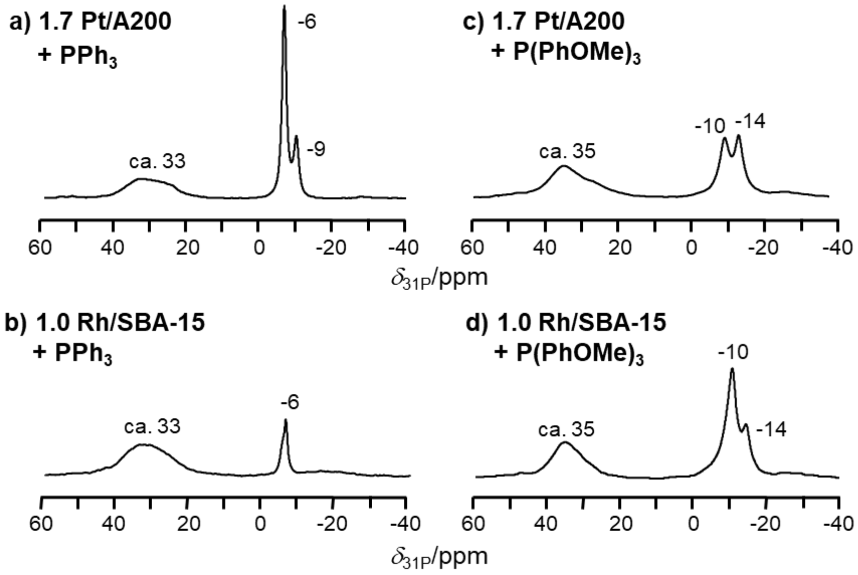

a) 1.7 Pt/A200 + PPh_3

c) 1.7 Pt/A200 + $P(PhOMe)_3$

b) 1.0 Rh/SBA-15 + PPh_3

d) 1.0 Rh/SBA-15 + $P(PhOMe)_3$

Fig. 3

In contrast, upon adsorption of $P(PhOMe)_3$ on platinum- and rhodium-loaded zeolites Na-Y, no ^{31}P MAS NMR signals of complexes occur at δ_{31P} ca. 35 ppm, while complex formation with PPh_3 is indicated by signals at δ_{31P} ca. 33 and 41 ppm is indicated (compare left- and right-hand side of **Fig. 4** shown below and Fig. 3 in Ref. [1]). This observation additionally evidences that $P(PhOMe)_3$ is too large for forming complexes with noble metal atoms located in the pores and cages of zeolite Y. Since the pore and cage system of zeolite Y is characterized by 12-ring windows with a diameter of 0.74 nm, which is one of the largest of common microporous zeolites, also the complex formation of $P(PhOMe)_3$ with noble metal inside the pores and cages of other zeolites can be excluded.

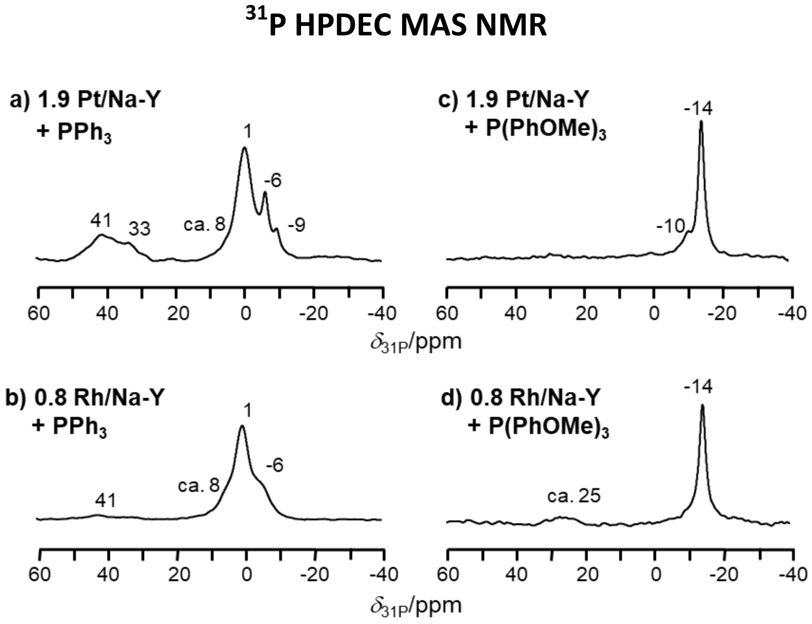

Fig. 4

A summary of the above-mentioned ^{31}P chemical shift values of bulk and physisorbed $P(PhOMe)_3$ as well as complexes of $P(PhOMe)_3$ with noble metals is given in Table 1 shown below. Considering these values, the **location of noble metals on the outer surface of zeolites can be determined by** formation of complexes with $P(PhOMe)_3$ leading to **signals at δ_{31P} ca. 35 ppm**. Contact of H_2-reduced noble metal-containing catalysts under study with oxygen (e.g. air) must be strictly avoided. Otherwise, oxidation of $P(PhOMe)_3$ can occur, leading to ^{31}P MAS NMR signals with chemical shifts near the range of signals due to complex formation with noble metals (line 4 of **Table 1**).

δ_{31P} / ppm	Assignment of $P(PhOMe)_3$ species
-14	bulk $P(PhOMe)_3$
-10	physisorbed $P(PhOMe)_3$ on open surfaces and in mesopores
ca. 25	decomposed oxidation products of $P(PhOMe)_3$
ca. 35	$[P(PhOMe]_nNM$ complexes on open surfaces and in mesopores

Table 1

For the quantitative evaluation of the ^{31}P MAS NMR signal intensities of noble metal complexes with phosphines, the procedure described by Equ. (3) of Section “method 12” is utilized. As an intensity standard, a well-known aluminosphosphate-type zeolite, such as VPI-5, is suitable. In this case, the repetition times t_{rep} of the ^{31}P MAS NMR measurements can be optimized by solely evaluating the ^{31}P MAS NMR signals of phosphines complexed with noble metals, recorded with t_{rep} = 20 s, while the VPI-5 standard is recorded with t_{rep} = 240 s. Phosphines physisorbed at the support surfaces without noble metals in their vicinity have much higher T_1 relaxation times compared with phosphines involved in complex formation with noble metals.

If $P(PhOMe)_3$ is applied together with PPh_3 (see Section “method 21”) as a molecular probe for the study of the spatial distribution of noble metals on zeolite Y, the noble metal locations summarized in **Table 2** (Table 4 in Ref. [1]) and visualized in **Fig. 5** can be distinguished by their complex formation with phosphines. Ref. [6] gives a survey on the above-mentioned topics.

Positions in Fig. 5	Noble metal location	Complexation with phosphines	^{31}P MAS NMR signal (ppm)
1	on outer particle surface of DeA-Y and Na-Y	PPh_3 and $P(PhOMe)_3$	ca. 33 and 35
2	in secondary mesopores of DeA-Y	PPh_3	ca. 33
3	in supercages (SII position) of Na-Y	PPh_3	41
4	in sodalite cages (SII’ position)	no	no
5	in hexagonal prisms (SI position)	no	no

Table 2

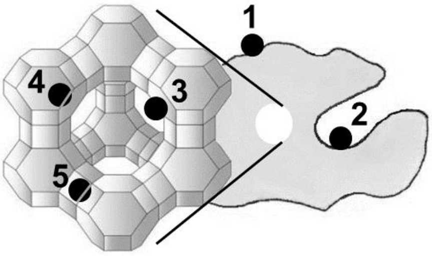

Fig. 5

Catalyst preparation: The noble metal-containing catalysts, prepared as described in Refs. [1-5], were calcined in synthetic air (970 mL/min) by heating with a rate of 2 K/min up to 573 K and further calcined at this temperature for 3 h, excluding the Ru-containing support materials. The materials were reduced in flowing hydrogen (100 mL/min) at 623 K (Pt-, Rh-, Pd-containing samples) or at 673 K (Ru-containing samples) for 2 h, transferred into glass tubes inside a glove box under nitrogen atmosphere, evacuated ($p < 10^{-2}$ Pa) at a vacuum line (see Section „vacuum line 1“ via link “*In Situ* Solid-State NMR Techniques”) at 298 K for 12 h, and sealed in glass tubes until their use.

For studies as those demonstrated in Figs. 2 to 4, loading of the H_2-reduced catalysts with tris(methoxyphenyl)phosphine ($P(PhOMe)_3$) of Sigma-Aldrich is performed by mixing of ca. 50 mg catalyst with ca. 10 mg $P(PhOMe)_3$ inside a rotor using e.g. a mini glove box purged with dry nitrogen gas (see Section “mini glove box” via link “*In Situ* Solid-State NMR Techniques”). Subsequently, the rotor is sealed with an O-ring-containing TORLON cap and heated at 433 K for 2 h for reaching a proper distribution of the $P(PhOMe)_3$ on the catalyst.

^{31}P MAS NMR studies: ^{31}P MAS NMR measurements were carried out using a Bruker Avance III 400WB spectrometer at a resonance frequency of 161.9 MHz using a 4 mm MAS NMR probe with sample spinning rates of 10 kHz. The spectra of the $P(PhOMe)_3$-loaded noble metal containing catalysts are recorded upon single pulse $\pi/2$ excitation with the repetition time of 20 s and high-power proton decoupling (HPDEC). The intensity standard VPI-5 is measured with a repetition time of 240 s. Chemical shifts are referenced to 0.85 M H_3P0_4 ($\delta_{31P} = 0$ ppm).

References:

[1] C. Rieg, D. Dittmann, Z. Li, D. Estes, M. Buchmeiser, M. Dyballa, M. Hunger, *Noble metal distribution on porous supports determined by reaction with phosphines*, Microporous & Mesoporous Mater. 310 (2021) 110594, DOI: 10.1016/j.micromeso.2020.110594.

[2] M. Dyballa, C. Rieg, D. Dittmann, Z. Li, M. Buchmeiser, B. Plietker, M. Hunger, *Potential of triphenylphosphine as solid-state NMR probe for studying the noble metal distribution on porous supports*, Microporous & Mesoporous Mater. 293 (2020) 109778, DOI: 10.1016/j.micromeso. 2019.109778.

[3] U. Obenaus, M. Dyballa, S. Lang, M. Scheibe, M. Hunger, *Generation and properties of Broensted acid sites in bifunctional Rh-, Ir-, Pd-, and Pt-containing zeolites Y investigated by solid-state NMR spectroscopy*, J. Phys. Chem. C 119 (2015) 15254-15262, DOI: 10.1021/acs.jpcc.5b03149.

[4] U. Obenaus, F. Neher, M. Scheibe, M. Dyballa, S. Lang, M. Hunger, *Relationships between the hydrogenation and dehydrogenation properties of Rh-, Ir-, Pd-, and Pt-containing zeolites Y studied by in situ MAS NMR spectroscopy and conventional heterogeneous catalysis*, J. Phys. Chem. C 120 (2016) 2284-2291, DOI: 10.1021/acs.jpcc.5b11367.

[5] U. Obenaus, S. Lang, R. Himmelmann, M. Hunger, *In situ MAS NMR investigation of parahydrogen induced hyperpolarization inside meso- and micropores of Ir-, Pt-, Rh-, and Pd-containing solid catalysts*, J. Phys. Chem. C 121 (2017) 9953-9962, DOI: 10.1021/acs.jpcc.7b01899.

[6] M. Dyballa, *Solid-State NMR Probe Molecules for Catalysts and Adsorbents: Concepts, Quantification, Accessibility, and Spatial Distribution*, Energy & Fuels 37(23) (2023) 18517-18559, DOI: 10.1021/acs.energyfuels.3c03815.